TEST Engineering & Management

January - February 2020
ISSN: 0193 - 4120 Page No. 11289 - 11295

Hyper Spectral Image Denoising via Sparse Representations over Learned Dictionaries

Dr. R. Sudheer Babu[1], Dr. S. Saheb Basha[2], L. Lakshmi Prasanna Kumar[3]

[1]Associate Professor, Electronics and Communication Engineering, G.Pulla Reddy Engineering College (Autonomous), Kurnool-5218007, A.P, India, email: sudheergprec@gmail.com

[2]Professor,Electronics and Communication Engineering, G.Pulla Reddy Engineering College (Autonomous), Kurnool-5218007, A.P, India, email: sahebshaik@gmail.com

[3]Assistant Professor,Electronics and Communication Engineering, G.Pulla Reddy Engineering College (Autonomous), Kurnool-5218007, A.P, India, email: lankek@gmail.com

Article Info
Volume 82
Page Number: 11289 - 11295
Publication Issue:
January-February 2020

Article History
Article Received*: 18 May 2019*
Revised*: 14 July 2019*
Accepted*: 22 December 2019*
Publication*: 21 February 2020*

Abstract
Hyperspectral pictures ar corrupted by noise throughout their acquisition and Hyperspectral image (HSI) denoising may be a crucial preprocessing procedure to enhance the performance of the following HSI interpretation and applications. In an HSI, there's an oversized quantity of native and international redundancy in its abstraction domain that may be wont to preserve the main points and texture. additionally, the correlation of the spectral domain is another valuable property that may be used to get smart results. during this work, we have a tendency to propose to expeditiously denoise hyperspectral pictures underneath the idea that the image patches ar thin in an exceedingly correct illustration domain outlined through a lexicon. we have a tendency to propose to rather learn the lexicon from Hyperspectral pictures, a task unremarkably referred to as lexicon learning. variety of HSI knowledge sets are employed in our analysis experiments and that we show that the lexicon learning approach is additional economical to denoise hyperspectral pictures than state-of the- art HSI denoising strategies with mounted dictionaries, at the price of a bigger computation time.

Keywords: *Hyperspectral image, denoising, sparsity, dictionary learning, K-SVD.*

1. INTRODUCTION

Unlike a typical image that aims to emulate human sight with solely 3 channels (red, green, and blue), hyperspectral pictures sit down with any image with significantly additional channels. whereas this variety isn't well outlined, a picture on the order of ten channels would be said as multispectral, whereas thirty one channels or higher is typically said as hyperspectral. These channels correspond to slim, equally spaced, wavelengths of sunshine. this extra spectral data may be priceless for several pc vision tasks like segmentation, and object classification. In part, this is often thanks to metameres; 2 objects could seem to own identical color to the human eye

whereas having considerably completely different responses at every wavelength of sunshine. whereas completely different, once these wavelengths ar combined into Associate in Nursing RGB or grayscale image they will seem identical. Consequently, it's not possible to extract hyperspectral information from Associate in Nursing RGB image while not further data.In the past decades, several algorithms are projected for noise reduction in HSI. a straightforward plan is to adopt a traditional denoising methodology for natural pictures band-by-band or pixel-by-pixel. However, these ways cannot get satisfactory

January - February 2020
ISSN: 0193 - 4120 Page No. 11289 - 11295

results as a result of they ignore the spectral correlation between completely different bands, that is of nice importance for rising denoising quality.

At an equivalent time, the spectral correlation is destroyed by the higher than ways and produces further distortion. Hence, the spatial and spectral dimensions ought to be thought of at the same time. Othman and Qian projected a noise reduction theme employing a riffle shrinkage primarily based hybrid spatial-spectral by-product domain during which the background level is elevated. the strategy utilised the difference of signal regularity within the corresponding spatial and spectral dimensions [7]. forward that the image noise exists within the low-energy principal part analysis (PCA) channels, bird genus and Qian projected a denoising rule supported PCA and wavelets [8]. In their rule, second quantity riffle thresholding is employed to get rid of the noise in low-energy PCA channels and a 1D dual-tree complicated riffle remodel (DCWT) primarily based denoising methodology is used to get rid of the spectrum noise of the HSI information cube.

Recently, distributed illustration (SR) primarily based ways are attracting additional attention in image denoising as a strong previous model [12–14]. within the SR framework, the signal is assumed to be delineate by a liner combination of a number of atoms during a learned or designed lexicon. supported this viewpoint, actuality signal may be recovered from its uproarious observation with Associate in Nursing ill-posed inverse downside by imposing the scantness previous. Rasti et al. projected a replacement liner model that sculptured the HSI with singular worth decomposition and wavelets so reconstructed actuality image supported distributed regularization [7]. This approach achieves some visual improvement and may be applied to giant information sets. In [2], a distributed low rank model for HSI was wont to solve the denoising downside. the 2 advantages of the projected model ar spatiality reduction with PCA and therefore the exploitation of DCWT coefficients associated with the principle components separately.

For the most part the techniques that we will investigate rely on similar principles which based on the characteristics of hyper spectral images previously examined by Chakrabartiet. al[11]. The most important characteristic being spectral similarityin local, spatial patches. Put another way, although we cannot say anything about the spatial similarity in x or y dimension, for small regions of natural scenes the spectral, !, dimension will exhibit a large amount of structure. This is the key to methods such as 3D dictionaries, which build dictionaries from patches with small spatial dimensions but full spectral dimensions, and tensor decomposition method swhich can approximate this spectral structure with a tensor of much lower spectral rank.

Here 10 patches were chosen at random from the same three images and factorized with varying spectral ranks. In this case we can clearly see the relationship between spectral rank and reconstruction quality and that we are able to achieve a better fit in smaller patches compared to

those of an entire image. We can now also see a direct relationship between rank and reconstruction. As previously mentioned, the spectral rank can be considerably reduced while maintaining a high quality representation of the patch. Only at a rank3 approximation do we begin to see a drastic fall in reconstruction quality.

2. SPARSE AND LOW-RANK MODELING

In this paper we focus on real world, visible spectrum hyper spectral images. Typically these are composed of 31 evenly spaced channels from 400nm to 700nm. While there are several data sets that match this criteria, for our purposes we have combined data from the Harvard[11], Stanford[21], Columbia[22], and Manchester[23] sets. These sets were chosen for their quality, variety of images, and their real world setting (i.e.,non satellite or GIS image data). From these images we discarded those with any masked data and randomly selected 50 images for training data and 3 quasi-randomly for testing. The testing set was generated by randomly selecting 3 images with the constraint that there be an outdoor scene, a natural scene, and that each image was from a different data set.

January - February 2020
ISSN: 0193 - 4120 Page No. 11289 - 11295

$$\mathbf{H} = \mathbf{X} + \mathbf{N} \quad (1)$$

where $\mathbf{H} \in R^{nx\ p}$ (with $n = n_1 n_2$) containing as its j^{th}column the vectorized observed image at band j. **X** and **N**are respectively the noise-free unknown signal, and the noisematrix, both (n x p) matrices.

2.1. Low-rank assumption

An HSI **X** is commonly modeled as a low-rank matrix in the literature [3, 11]. The classical linear There are two main dictionary parameters which a↵ect the speed and quality of reconstruction. The first being the patch size of the dictionary which controls the number of pixels along x and y, as well as the number of wavelength channels long !.There are no restrictions on the sizes of patches, however, as discussed in section 2 smaller patches will result in higher quality reconstructions while also increasing thetime required to find a solution.

$$\mathbf{H} = \boldsymbol{U} \sum \boldsymbol{V^T} + \mathbf{N} \quad (2)$$

where the columns of $\mathbf{U},\mathbf{V} \in R^{n\ x\ r}$ are respectively a setof vectorized Eigen-images and the associated spectral components,and $\sum \in R^{r\ x\ r}$ is a diagonal singular value matrix.

2.2. Sparsity assumption

The second parameter is referred to as the over completeness factor. This value controls the number of dictionary elements learned and used during reconstruction.A complete dictionary refers to a dictionary with as many dictionary elements as

elements in a single patch of the dictionary. A dictionary with an over completeness factor of two would therefore have twice as many patches as pixel elements per patch. Increasing this factor will also increase computation time and memory requirements.

$$\mathbf{H} = \mathbf{BW}\sum \mathbf{V^T} + \mathbf{N} \quad (3)$$

3.PROPOSED APPROACH

A first part of our contribution consists in replacing the classicorthogonal Wavelet basis in the described pipeline by adictionary both 1) overcomplete and 2) learned from data.

3.1. Over complete learned dictionary

Unlike the other methods we discuss, TDL learns its dictionary online and thus requires no dictionary to be learned before use. Therefore, we may simply evaluate itsperformance on all three of our noisy test scenes. For best results we use the providedcode and recommended parameters provided by the authors, varying only the size ofthe patches used during reconstruction. For the sake of comparison we chose patchsizes in the same range as those used for the 3D patch based dictionary described in

Section 3.

1. K-SVD [9] as a standard (baseline) algorithm for learnin gun structured dictionaries;

2. SuKro [10] as an algorithm for learning Kronecker structured dictionaries.

This assessment is also corroborated by comparing per-pixel sum of errors between algorithms. Whereas the 3D Dictionary errors appear to be largely due to Poisson noise peaks, the TDL algorithm was able to remove this noise at th eexpense of fine detail. Finally, we can also see the e↵ect of tensor decomposition inthe resulting image by way of banding artifacts in individual patches which haven't been compensated for by averaging overlapping pixels. Unlike the 3D Dictionary, the per-wavelength error (as shown in Figure 4.10) is significantly di↵erent for each input scene. Much like the 3D Dictionary however, thiserror is caused by the mean of the training data which, as this is an online dictionary learning tool, is the input test scene itself. Nevertheless, as we can see in Figure 4.17,all three scenes' errors correspond directly to their mean.

3.2. A patch-based denoising approach

Recent advances, such as the work by Bristow et. al [9], and Heide et. al [10], have moved convolutional sparse coding (CSC) into the spotlight for a number of machine learning and computer vision tasks. Similar to spatial image dictionaries explored in Chapter 3, a dictionary of patches is learned that can be used to represent any image. In this case, however, the patches are convoluted with a sparse image scalebasis. In addition to being faster, these creates image scale

January - February 2020
ISSN: 0193 - 4120 Page No. 11289 - 11295

features eliminate patchsizedarti facts that often appear in spatial patch dictionaries.

$$\{\widehat{D}, \Gamma\} = argmin_{D,\Gamma} \|D\Gamma - Y\|_F^2 + g(\Gamma) \quad (4)$$

While these methods have proved quite e↵ective for greyscale images, currentlythere has been no work investigating their application to hyperspectral data sets.In this section we provide some preliminary investigations and results of our workextending CSC to hyperspectral images and its current limitations.

3.3. Dictionary Learning Algorithms

There are several possible ways to extend CSC along a third dimensions. First, it would be possible to learn 3D feature patches and to treat x, d, and z as rank three tensors, applying ⇤←as a 3D convolution. However, due to the structure of hypers pectraldata, and the considerably reduced rank along the wavelength dimension, there is little reason to believe image scale structure, similar to those found along the spatial dimensions, would be exploitable in as few as 31 bands.

4. EXPERIMENTAL RESULTS

Although our method solves for all dictionary kernels and coefficients simultaneously, it lacks any constraint requiring each wavelength from a dictionary kernel to be use data given coefficient position. In this chapter we show how we can exploit the construction of the dictionary to impose this type of solution automatically. While there are many ways to initialize our dictionary and coefficients during the dictionary learning process, here we emphasize two specific scenarios. The first, referred to from now on as all random initialization, describes a dictionary which was initialized with random variables for all coefficient and kernel values across all wave lengths. The second, referred to from now on as repeated random initialization, describes a dictionary for which one wavelength's coefficients and kernels were randomly initialized and then repeated for each additional channel.

Second, in Figure 2.2 we see the average reconstruction quality for patches of sizes ranging from 2 →⇥2 to 64 →⇥64 spatial pixels. Here 10 patches were chosen atrandom from the same three images and factorized with varying spectral ranks. In this case we can clearly see the relationship between spectral rank and reconstruction quality and that we are able to achieve a better fit in smaller patches compared tothose of an entire image. We can now also see a direct relationship between rank and reconstruction. As previously mentioned, the spectral rank can be considerably reduced while maintaining a high quality representation of the patch. Only at a rank3 approximation do we begin to see a drastic fall in reconstruction quality.

Unfortunately, this assumption does not hold under the presence of significant noise. As additional noise is added to the image over fitting can become a real concern for smaller patches. Increasing the size of the patches used for reconstruction results in more outliers being smoothed. While reconstructions performed with larger patches are less faithful to the noisy data, they better represent the intrinsic image. Again this is shown in Figures 2.3 and 2.4, where we compare average patch reconstruction of the noisy input image when compared to the intrinsic image as opposed to itself.

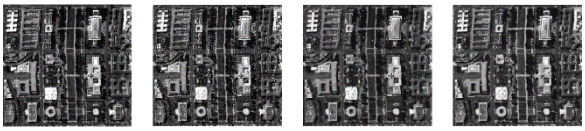

Figure 1. 1st Spectral band of Original Image, Noisy Image, SuKro, HyRes

January - February 2020
ISSN: 0193 - 4120 Page No. 11289 - 11295

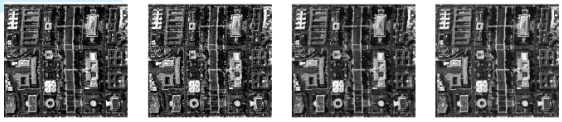

Figure 2. 123rd Spectral band of Original Image, Noisy Image, SuKro, HyRes

Table 1. Output SNR [dB] Comparison with literature

	Method	Input SNR [dB]					
		5	10	15	20	25	30
San Diego	Wave.3D	20.19	23.36	26.51	29.48	32.33	35.08
	HyRes	23.26	26.37	29.63	32.61	35.44	37.92
	ODCT	24.79	27.77	30.79	33.77	36.57	38.88
	K-SVD	24.92	27.86	30.89	33.88	36.68	39.00
	SuKro	24.95	27.93	30.94	33.89	36.69	38.99
Houston	Wave.3D	18.28	21.59	24.90	28.19	31.45	34.64
	HyRes	22.86	26.45	29.76	33.00	36.08	39.49
	ODCT	24.18	27.49	30.87	34.13	37.30	39.85
	K-SVD	24.38	27.64	31.01	34.27	37.45	39.99
	SuKro	24.39	27.63	30.98	34.23	37.42	39.97

Table 2. Execution times (in seconds) for San Diegoimage

	Method	Input SNR [dB]					
		5	10	15	20	25	30

January - February 2020
ISSN: 0193 - 4120 Page No. 11289 - 11295

San Diego	Wave.3D	125	120	125	125	120	124
	HyRes	55	50	50	49	48	50
	ODCT	128	201	296	408	533	761
	K-SVD	273	445	677	980	1315	1650
	SuKro	262	394	592	857	1143	1433

5. CONCLUSION

In this paper, we proposed to replace fixed transforms by over complete learned dictionaries to improve state-of- the-art performance in the HSI denoising task. Although the proposed patch-based approach is markedly slower than other previous methods, running times remain reasonable for an offline application, even for large images.

REFERENCES

[1] P. S. Thenkabail, J. G. Lyon, and A. Huete, Hyperspectral remote sensing ofvegetation. CRC Press, 2011.

[2] G. ElMasry, N. Wang, A. ElSayed, and M. Ngadi, "Hyperspectral imaging fornondestructive determination of some quality attributes for strawberry," Journalof Food Engineering, vol. 81, no. 1, pp. 98–107, 2007.

[3] O. Y. Rodionova, L. P. Houmøller, A. L. Pomerantsev, P. Geladi, J. Burger,V. L. Dorofeyev, and A. P. Arzamastsev, "Nir spectrometry for counterfeit drugdetection: a feasibility study," AnalyticaChimicaActa, vol. 549, no. 1, pp. 151–158, 2005.

[4] A. Wagadarikar, R. John, R. Willett, and D. Brady, "Single disperser design forcoded aperture snapshot spectral imaging," Applied optics, vol. 47, no. 10, pp.B44–B51, 2008.

[5] X. Lin, Y. Liu, J. Wu, and Q. Dai, "Spatial-spectral encoded compressive hyperspectralimaging," ACM Transactions on Graphics (TOG), vol. 33, no. 6, p.233, 2014.

[6] M. Goel, E. Whitmire, A. Mariakakis, T. S. Saponas, N. Joshi, D. Morris,B. Guenter, M. Gavriliu, G. Borriello, and S. N. Patel, "Hypercam: hyperspectralimaging for ubiquitous computing applications," in Proceedings of the 2015ACM International Joint Conference on Pervasive and Ubiquitous Computing.ACM, 2015, pp. 145–156.

[7] N. Akhtar, F. Shafait, and A. Mian, "Bayesian sparse representation for hyperspectralimage super-resolution," in IEEE Conf. on Computer Vision and Pattern Recognition (CVPR), 2015.

[8] L. Wang, Z. Xiong, D. Gao, G. Shi, W. Zeng, and F. Wu, "High-speed hyperspectral video acquisition with a dual-camera architecture," in Proceedings of The IEEE Conference on Computer Vision and Pattern Recognition, 2015, pp.4942–4950.

[9] H. Bristow, A. Eriksson9. M. Aharon, M. Elad, and A. Bruckstein, "K-SVD: An algorithm for designing overcomplete dictionaries for sparse representation," IEEE Transactions on Signal Processing, vol. 54, no. 11, Nov 2006.

[10] C. F. Dantas, M. N. da Costa, and R. d. R. Lopes, "Learning dictionaries as a sum of kronecker products," IEEE Signal Processing Letters, vol.24, no. 5, pp. 559–563, May 2017.

[11] Dabov, K.; Foi, A.; Katkovnik, V.; Egiazarian, K. Image Denoising by Sparse 3-D Transform-Domain Collaborative Filtering. IEEE Trans. Image Process. 2007, 16, 2080.

[12] Rudin, L.I.; Osher, S.; Fatemi, E. Nonlinear total variation based noise removal algorithms. Phys. D NonlinearPhenom. 1992, 60, 259–268.

[13] Buades, A.; Coll, B.; Morel, J.M. A Non-Local Algorithm for Image Denoising. In Proceedings of the 2005 IEEE Computer Society Conference on Computer Vision and Pattern Recognition, San Diego, CA, USA, 20–25 June 2005; pp. 60–65.

[14] Dabov, K.; Foi, A.; Egiazarian, K. Video denoising by sparse 3D transform-domain collaborative filtering. In Proceedings of the 2007 European Signal Processing Conference,

January - February 2020
ISSN: 0193 - 4120 Page No. 11289 - 11295

Poznan, Poland, 3–7 September 2007; pp. 145–149.

[15] Maggioni, M.; Katkovnik, V.; Egiazarian, K.; Foi, A. A Nonlocal transform-domain filter for volumetric data denoising and reconstruction. IEEE Trans. Image Process. 2013, 22, 119–133.